

Fully Implicit Discontinuous Galerkin Schemes for Multiphase Flow

Y.Epshteyn and B.Rivière¹

Department of Mathematics, University of Pittsburgh, 301 Thackeray, Pittsburgh, PA 15260, U.S.A.

Abstract

In this paper we formulate two numerical methods for modeling two-phase flow problems arising in porous media. The unknowns are approximated by piecewise discontinuous polynomials of arbitrary high degree. No postprocessing, such as slope limiters, is needed. The Jacobian matrix for the Newton-Raphson scheme, is given. Numerical examples of homogeneous and heterogeneous media are presented.

Key words: nonsymmetric interior penalty Galerkin, h and p-version, Newton-Raphson, heterogeneous media

1 Introduction

The understanding of multiphase flow is of crucial importance to agencies concerned with energy, in particular oil production. This paper deals with the modeling of two-phase flow, for example the flow of a wetting phase (such as water) and a non-wetting phase (such as dense non-aqueous phase liquids), in a porous medium with possibly heterogeneous characteristics. This type of flow is mathematically modeled by a nonlinear system of coupled partial differential equations (PDEs) that express the conservation laws of mass and momentum and that in general can only be solved by the use of numerical methods. A review on the issues arising in modeling multiphase flow is given in [10].

Affordable computing power allows oil engineers to add complexity to their reservoir models. Some of the features that may have been ignored previously include for instance, complex geometry, faults, channels and deviated wells.

¹ University of Pittsburgh, Central Research Development Fund, 2004-39742

It is therefore important to develop discretization methods that approximate accurately physical quantities such as pressure, flow rates and mass balances on highly unstructured and non-conforming grids. The current industrial reservoir simulators support finite differences, which are quite popular and efficient on regular structured grids [13]. But, these methods can lose their stability on unstructured meshes and are not ideal for complex geometries.

The goal of this paper is to introduce a high order discontinuous Galerkin (DG) method for solving incompressible two-phase problem. Over the last few years, discontinuous finite element methods have been shown to be competitive with respect to other standard techniques in flow and transport problems: they have been successfully applied to single phase flow, miscible displacement and linear transport [17,14,16,15,6]. The appeal of these methods lies in their local behavior: the mesh can be locally refined, the degree of polynomial approximation can vary from grid cell to grid cell, and the mass balance equations are satisfied elementwise. The method introduced here is based on the Non-symmetric Interior Penalty Galerkin (NIPG) method introduced and analyzed in [17] for diffusion problems. A variety of DG methods are described in [4].

In this work we consider two different implicit pressure-saturation formulations for two-phase flow. The primary variables are the pressure of the wetting phase and the saturation of the non-wetting phase. They are approximated by discontinuous polynomials of different degrees. The resulting finite dimensional problem is an algebraic system of nonlinear equations to which the Newton-Rapshon iterative scheme is applied. **No slope-limiter techniques are employed.** A detailed description of several models of multiphase flow can be found in [7,11,8]. In [12,1], DG methods are applied to a sequential pressure-saturation formulation, in which the coefficients are evaluated at the previous time step. In this case, overshoot and undershoot occur and they are removed by the use of slope limiters [3,5]. Some of the difficulties of slope limiters are the lack of theoretical convergence in two or three dimensions.

The outline of the paper is as follows. Section 2 contains the description of the two formulations of the model problem. The fully implicit numerical scheme is introduced in Section 3. In Section 4 the Newton-Rapshon algorithm applied to the resulted system of the nonlinear equations is considered and construction of the jacobian is given. Numerical results for homogeneous and heterogeneous permeability fields are given in Section 5. Conclusions follow.

2 Model Problem.

Let Ω be a polygonal porous medium in \mathbb{R}^2 . The flow of the wetting phase (such as water) and non-wetting phase (such as oil) in Ω is described by Darcy's law and the continuity equation for each phase. Let us denote by the subscript $\alpha = w$ and $\alpha = n$ the wetting and non-wetting phase respectively. The Darcy velocity for each phase is given by :

$$u_\alpha = -\lambda_\alpha K \nabla p_\alpha, \quad \alpha = w, n, \quad (1)$$

where p_α is the phase pressure, and the continuity equation satisfied by the phase saturation s_α is given by

$$\frac{\partial(\rho_\alpha \phi s_\alpha)}{\partial t} + \nabla \cdot (\rho_\alpha u_\alpha) = \rho_\alpha q_\alpha, \quad \alpha = w, n. \quad (2)$$

The coefficients in (1) and (2) are defined below:

- The permeability K is a symmetric positive definite tensor, obtained from a macroscopic averaging of the microscopic features of the medium. Hence, it can be discontinuous in the space variable and can vary over several orders of magnitude.
- λ_w and λ_n are the mobilities of the wetting and non-wetting phase respectively. Mobilities are the ratios of relative permeabilities by the viscosities

$$\lambda_\alpha = \frac{k_{r\alpha}}{\mu_\alpha}, \quad \alpha = w, n, \quad (3)$$

and the relative permeabilities are functions that depend on the non-wetting phase saturation s_n in a non-linear fashion. In this work, the commonly used Brooks-Corey model [2] is considered.

$$k_{rw}(s) = (1 - s)^{\frac{2+3\theta}{\theta}}, \quad k_{rn}(s) = s^2(1 - (1 - s)^{\frac{2+\theta}{\theta}}). \quad (4)$$

This model introduces an additional parameter $\theta \in [0.2, 3.0]$, which characterizes the inhomogeneity of the medium. We also denote $\lambda_t = \lambda_w + \lambda_n$ the total mobility.

- In addition to Equations (1) and (2), the following closure relations must also be satisfied:

$$s_w + s_n = 1, \quad (5)$$

$$p_c = p_n - p_w, \quad (6)$$

where p_c is the capillary pressure given by:

$$p_c(s) = p_d(1 - s)^{-\frac{1}{\theta}}. \quad (7)$$

Here, p_d is the capillary pressure needed to displace the fluid from the largest pore.

- ρ_α, ϕ are the phase densities and porosity respectively.

We have restricted our consideration to incompressible fluid flow, i.e. the densities ρ_α are constant. Furthermore, we assume that the porosity ϕ is constant over the entire domain. Under these assumptions, the continuity equation (2) is reduced to

$$\phi \frac{\partial s_\alpha}{\partial t} + \nabla \cdot (u_\alpha) = q_\alpha, \quad \alpha = w, n. \quad (8)$$

The continuity equation (8) and Darcy's law (1) is the basis for the description of incompressible multiphase flow processes. The pressure and saturation can be coupled using the closure relations (5) and (6). In this paper, we consider two formulations of the two-phase flow problem, described below.

The first formulation of the model for the coupled pressure-saturation equations for incompressible two-phase flow with unknowns p_w and s_n can be derived by summing continuity equations (8) for wetting and non-wetting phase and using (1), (5), (6) and continuity equation (8) for wetting phase:

$$\begin{aligned} -\nabla \cdot (\lambda_t K \nabla p_w + \lambda_n K \nabla p_c) &= q_w + q_n, \\ -\phi \frac{\partial s_n}{\partial t} - \nabla \cdot (\lambda_w K \nabla p_w) &= q_w. \end{aligned} \quad (9)$$

The second formulation of the model for the coupled pressure-saturation equations for incompressible two-phase flow with unknowns p_w and s_n can be obtained by substituting (1), (5), (6) into (8) :

$$\begin{aligned} -\phi \frac{\partial s_n}{\partial t} - \nabla \cdot (\lambda_w K \nabla p_w) &= q_w, \\ \phi \frac{\partial s_n}{\partial t} - \nabla \cdot (\lambda_n K (\nabla p_c + \nabla p_w)) &= q_n. \end{aligned} \quad (10)$$

Both formulations of the coupled pressure-saturation equations stated above are subject to the following boundary and initial conditions. We assume that boundary of the domain is divided into three disjoint open sets $\partial\Omega = \Gamma_N \cup \Gamma_+ \cup \Gamma_-$ and we denote by n the outward normal to the $\partial\Omega$.

$$\begin{aligned} p_w &= p_{dir}^-, \quad s_n = s_n^{dir}, \quad \text{on } \Gamma_- \text{ - the inflow boundary,} \\ p_w &= p_{dir}^+, \quad \lambda_n K \nabla p_c \cdot n = 0, \quad \text{on } \Gamma_+ \text{ - the outflow boundary,} \\ \lambda_w K \nabla p_w \cdot n &= 0, \quad \lambda_n K \nabla p_n \cdot n = 0, \quad \text{on } \Gamma_N \text{ - no-flow boundary,} \end{aligned} \quad (11)$$

$$s_n(\Omega; 0) = s^0(\Omega), \quad \text{saturation at time } t = 0. \quad (12)$$

The systems of partial differential equations for formulations (9) and (10) can be classified as mixed hyperbolic-parabolic type and these formulations are numerically investigated in the rest of the paper.

3 Fully Implicit Scheme

The domain Ω is subdivided into a non degenerate quasi-uniform partition $\mathcal{E}_h = \{E\}_E$ consisting of N_h quadrilaterals of maximum diameter h . Let Γ_h be the union of the open sets that coincide with interior edges of elements of \mathcal{E}_h . Let e denote a segment of Γ_h shared by two elements E^k and E^l of \mathcal{E}_h ; we associate with e a unit normal vector n_e directed from E^k to E^l , ($k > l$), and we define formally the jump and average of a function ψ on e by :

$$[\psi] = (\psi|_{E^k})|_e - (\psi|_{E^l})|_e \quad (13)$$

$$\{\psi\} = \frac{1}{2}(\psi|_{E^k})|_e + \frac{1}{2}(\psi|_{E^l})|_e \quad (14)$$

If e is adjacent to $\partial\Omega$, then the jump and the average of ψ on e coincide with the trace of ψ on e and the normal vector n_e coincides with the outward normal n . We also denote by $|e|$ the length of e . For a given integer $r \geq 0$, the discontinuous finite element space is

$$\mathcal{D}_r(\mathcal{E}_h) = \{v \in L^2(\Omega) : v|_E \in \mathbb{P}_r(E) \quad \forall E \in \mathcal{E}_h\}, \quad (15)$$

where $\mathbb{P}_r(E)$ is the space of polynomials of total degree less than or equal to r . We approximate the pressure of the wetting phase and saturation of the non-wetting phase by discontinuous polynomials of total degrees r_p and r_s respectively.

The time interval is divided into N equal subintervals of length Δt . Let $t^i = i\Delta t$ and let p_w^i and s_n^i be the numerical solutions at time t^i . We also denote $\lambda_\alpha^i = \lambda_\alpha(s_n^i)$ and $p_c^i = p_c(s_n^i)$. Application of the backward Euler scheme for time stepping and NIPG for the space discretization to the system of PDEs for the coupled equations (9) and (10) yields two systems of nonlinear equations.

Fully implicit scheme for first formulation (9): given $(p_w^i, s_n^i) \in \mathcal{D}_{r_p}(\mathcal{E}_h) \times \mathcal{D}_{r_s}(\mathcal{E}_h)$, find (p_w^{i+1}, s_n^{i+1}) satisfying

Pressure Equation :

$$\begin{aligned} & \sum_{E \in \mathcal{E}_h} \int_E \lambda_t^{i+1} K \nabla p_w^{i+1} \cdot \nabla z + \sum_{E \in \mathcal{E}_h} \int_E \lambda_n^{i+1} K \nabla p_c^{i+1} \cdot \nabla z \\ & - \sum_{e \in \Gamma_h \cup \Gamma_{D^+} \cup \Gamma_{D^-}} \int_e \{\lambda_t^{i+1} K \nabla p_w^{i+1} \cdot n_e\} [z] - \sum_{e \in \Gamma_h \cup \Gamma_{D^-}} \int_e \{\lambda_n^{i+1} K \nabla p_c^{i+1} \cdot n_e\} [z] \\ & + \sum_{e \in \Gamma_h \cup \Gamma_{D^+} \cup \Gamma_{D^-}} \int_e \{\lambda_t^{i+1} K \nabla z \cdot n_e\} [p_w^{i+1}] + \sum_{e \in \Gamma_h \cup \Gamma_{D^-}} \int_e \{\lambda_n^{i+1} K \nabla z \cdot n_e\} [p_c^{i+1}] \end{aligned}$$

$$\begin{aligned}
& + \sum_{e \in \Gamma_h \cup \Gamma_{D^+} \cup \Gamma_{D^-}} \frac{\sigma_e^0}{|e|^\beta} \int_e [p_\omega^{i+1}][z] + \sum_{e \in \Gamma_h \cup \Gamma_{D^-}} \frac{\sigma_e^0}{|e|^\beta} \int_e [p_c^{i+1}][z] \\
& - \sum_{e \in \Gamma_{D^+} \cup \Gamma_{D^-}} \int_e (\lambda_n^{i+1} K \nabla z \cdot n_e) p_\omega^{dir} - \sum_{e \in \Gamma_{D^+} \cup \Gamma_{D^-}} \frac{\sigma_e^0}{|e|^\beta} \int_e p_\omega^{dir} z \\
& - \sum_{e \in \Gamma_{D^-}} \int_e (\lambda_n^{i+1} K \nabla z \cdot n_e) p_c(s_{dir}) - \sum_{e \in \Gamma_{D^-}} \frac{\sigma_e^0}{|e|^\beta} \int_e p_c(s_{dir}) z = 0, \quad \forall z \in \mathcal{D}_{r_p}(\mathcal{E}_h).
\end{aligned} \tag{16}$$

Saturation Equation :

$$\begin{aligned}
& - \int_\Omega \frac{\phi}{\Delta t} (s_n^{i+1} - s_n^i) v + \sum_{E \in \mathcal{E}_h} \int_E \lambda_\omega^{i+1} K \nabla p_\omega^{i+1} \cdot \nabla v - \sum_{e \in \Gamma_h \cup \Gamma_{D^+} \cup \Gamma_{D^-}} \int_e \{ \lambda_\omega^{i+1} K \nabla p_\omega^{i+1} \cdot n_e \} [v] \\
& + \sum_{e \in \Gamma_h \cup \Gamma_{D^+} \cup \Gamma_{D^-}} \int_e \{ \lambda_\omega^{i+1} K \nabla v \cdot n_e \} [p_\omega^{i+1}] + \sum_{e \in \Gamma_h \cup \Gamma_{D^+} \cup \Gamma_{D^-}} \frac{\sigma_e^0}{|e|^\beta} \int_e [p_\omega^{i+1}][v] \\
& - \sum_{e \in \Gamma_{D^+} \cup \Gamma_{D^-}} \int_e (\lambda_\omega^{i+1} K \nabla v \cdot n_e) p_\omega^{dir} - \sum_{e \in \Gamma_{D^+} \cup \Gamma_{D^-}} \frac{\sigma_e^0}{|e|^\beta} \int_e p_\omega^{dir} v = 0, \quad \forall v \in \mathcal{D}_{r_s}(\mathcal{E}_h),
\end{aligned} \tag{17}$$

where β is a positive constant and σ_e^0 are the penalties parameters on interior and boundary edges penalizing the jumps of the discontinuous polynomials.

Fully implicit scheme for second formulation (10): given $(p_\omega^i, s_n^i) \in \mathcal{D}_{r_p}(\mathcal{E}_h) \times \mathcal{D}_{r_s}(\mathcal{E}_h)$, find $(p_\omega^{i+1}, s_n^{i+1})$ satisfying

Pressure Equation :

$$\begin{aligned}
& \int_\Omega \frac{\phi}{\Delta t} (s_n^{i+1} - s_n^i) z + \sum_{E \in \mathcal{E}_h} \int_E \lambda_n^{i+1} K (\nabla p_\omega^{i+1} + \nabla p_c^{i+1}) \cdot \nabla z \\
& - \sum_{e \in \Gamma_h \cup \Gamma_{D^+} \cup \Gamma_{D^-}} \int_e \{ \lambda_n^{i+1} K \nabla p_\omega^{i+1} \cdot n_e \} [z] - \sum_{e \in \Gamma_h \cup \Gamma_{D^-}} \int_e \{ \lambda_n^{i+1} K \nabla p_c^{i+1} \cdot n_e \} [z] \\
& + \sum_{e \in \Gamma_h \cup \Gamma_{D^+} \cup \Gamma_{D^-}} \int_e \{ \lambda_n^{i+1} K \nabla z \cdot n_e \} [p_\omega^{i+1}] + \sum_{e \in \Gamma_h \cup \Gamma_{D^-}} \int_e \{ \lambda_n^{i+1} K \nabla z \cdot n_e \} [p_c^{i+1}] \\
& + \sum_{e \in \Gamma_h \cup \Gamma_{D^+} \cup \Gamma_{D^-}} \frac{\sigma_e^0}{|e|^\beta} \int_e [p_\omega^{i+1}][z] + \sum_{e \in \Gamma_h \cup \Gamma_{D^-}} \frac{\sigma_e^0}{|e|^\beta} \int_e [p_c^{i+1}][z] \\
& - \sum_{e \in \Gamma_{D^+} \cup \Gamma_{D^-}} \int_e (\lambda_n^{i+1} K \nabla z \cdot n_e) p_\omega^{dir} - \sum_{e \in \Gamma_{D^+} \cup \Gamma_{D^-}} \frac{\sigma_e^0}{|e|^\beta} \int_e p_\omega^{dir} z \\
& - \sum_{e \in \Gamma_{D^-}} \int_e (\lambda_n^{i+1} K \nabla z \cdot n_e) p_c(s_{dir}) - \sum_{e \in \Gamma_{D^-}} \frac{\sigma_e^0}{|e|^\beta} \int_e p_c(s_{dir}) z = 0, \quad \forall z \in \mathcal{D}_{r_p}(\mathcal{E}_h).
\end{aligned} \tag{18}$$

Saturation Equation :

$$\begin{aligned}
& - \int_{\Omega} \frac{\phi}{\Delta t} (s_n^{i+1} - s_n^i) v + \sum_{E \in \mathcal{E}_h} \int_E \lambda_{\omega}^{i+1} K \nabla p_{\omega}^{i+1} \cdot \nabla v - \sum_{e \in \Gamma_h \cup \Gamma_{D^+} \cup \Gamma_{D^-}} \int_e \{ \lambda_{\omega}^{i+1} K \nabla p_{\omega}^{i+1} \cdot n_e \} [v] \\
& + \sum_{e \in \Gamma_h \cup \Gamma_{D^+} \cup \Gamma_{D^-}} \int_e \{ \lambda_{\omega}^{i+1} K \nabla v \cdot n_e \} [p_{\omega}^{i+1}] + \sum_{e \in \Gamma_h \cup \Gamma_{D^+} \cup \Gamma_{D^-}} \frac{\sigma_e^0}{|e|^{\beta}} \int_e [p_{\omega}^{i+1}] [v] \\
& - \sum_{e \in \Gamma_{D^+} \cup \Gamma_{D^-}} \int_e (\lambda_{\omega}^{i+1} K \nabla v \cdot n_e) p_{\omega}^{dir} - \sum_{e \in \Gamma_{D^+} \cup \Gamma_{D^-}} \frac{\sigma_e^0}{|e|^{\beta}} \int_e p_{\omega}^{dir} v = 0, \quad \forall v \in \mathcal{D}_{r_s}(\mathcal{E}_h).
\end{aligned} \tag{19}$$

Because of the nonlinearity in equations (16),(17) and (18), (19), the approximations at the next time step (p_w^{i+1}, s_n^{i+1}) are obtained by applying Newton-Raphson iterative scheme [9], described in the next section.

4 Newton-Raphson iterative scheme and construction of the Jacobian

Assume that $\{\varphi_E^{l_s} : 1 \leq l_s \leq m_s, E \in \mathcal{E}_h\}$ and $\{\varphi_E^{l_p} : 1 \leq l_p \leq m_p, E \in \mathcal{E}_h\}$ are two basis for the discrete spaces $\mathcal{D}_{r_s}(\mathcal{E}_h)$ and $\mathcal{D}_{r_p}(\mathcal{E}_h)$ respectively. It is understood that the functions φ_E^i are identically zero outside the element E . Thus, we can write

$$s_n^{i+1}|_E = \sum_{l_s=1}^{m_s} s_E^{l_s} \varphi_E^{l_s}, \quad p_w^{i+1}|_E = \sum_{l_p=1}^{m_p} p_E^{l_p} \varphi_E^{l_p}, \quad \forall E \in \mathcal{E}_h. \tag{20}$$

Thus, inserting (20) into (16)-(19), we obtain systems of algebraic nonlinear equations in the general form of:

$$G(\bar{p}_w^{i+1}, \bar{s}_n^{i+1}) = 0, \tag{21}$$

where $\bar{p}_w^{i+1} = (p_E^{l_p})_{E, l_p}$ and $\bar{s}_n^{i+1} = (s_E^{l_s})_{E, l_s}$ are vectors of unknowns for p_w^{i+1} and s_n^{i+1} . To solve (21) we apply Newton-Raphson algorithm :

$$\begin{aligned}
J_G(\bar{p}_w^{i+1, r}, \bar{s}_n^{i+1, r}) \bar{\delta}^{r+1} &= -G(\bar{p}_w^{i+1, r}, \bar{s}_n^{i+1, r}), \\
(\bar{p}_w^{i+1, r+1}, \bar{s}_n^{i+1, r+1}) &= (\bar{p}_w^{i+1, r}, \bar{s}_n^{i+1, r}) + \bar{\delta}^{r+1},
\end{aligned} \tag{22}$$

where the superscript r denotes the r^{th} Newton-Raphson iterate and J_G is the Jacobian of the system (21). In order to explicitly define J_G we denote by $G_F^{k_p}$ (resp. $G_F^{k_s}$) the row of G corresponding to the test function $\varphi_F^{k_p}$ (resp.

$\varphi_F^{k_s}$), with $F \in \mathcal{E}_h$ and $1 \leq k_p \leq m_p$ (resp. $1 \leq k_s \leq m_s$). Then, we can write J_G in a block form:

$$J_G = \begin{pmatrix} \frac{\partial G_F^{k_p}}{\partial p_E^{l_p}} & \frac{\partial G_F^{k_p}}{\partial s_E^{l_s}} \\ \frac{\partial G_F^{k_s}}{\partial p_E^{l_p}} & \frac{\partial G_F^{k_s}}{\partial s_E^{l_s}} \end{pmatrix} \begin{matrix} 1 \leq k_p, l_p \leq m_p \\ 1 \leq k_s, l_s \leq m_s \end{matrix} .$$

$$E, F \in \mathcal{E}_h$$

In the derivation below, we separate the contributions to the Jacobian between contributions from volume integrals, interior edges and boundary edges. For the interior edge contribution associated to one edge e , we assume that e is shared by the elements E_1 and E_2 and for the boundary edge contribution, we assume that e belongs to E_1 . We also use the notation ξ^i for the restriction of any function ξ on the element E_i for $i = 1, 2$. We now give the computation of the nonzero entries for the block diagonal Jacobian for the scheme (16),(17). A similar derivation can be done for the scheme (18), (19).

Contribution from the pressure equation (16):

Volume integrals:

$$\frac{\partial G_E^{k_p}}{\partial p_E^{l_p}} = \int_E \lambda_t K \nabla \varphi_E^{l_p} \cdot \nabla \varphi_E^{k_p},$$

$$\begin{aligned} \frac{\partial G_E^{k_p}}{\partial s_E^{l_s}} &= \int_E \frac{\partial \lambda_t}{\partial s_E^{l_s}} \varphi_E^{l_s} K \nabla p_w \cdot \nabla \varphi_E^{k_p} + \int_E \frac{\partial \lambda_n}{\partial s_E^{l_s}} \varphi_E^{l_s} K \nabla p_c \cdot \nabla \varphi_E^{k_p} \\ &+ \int_E \lambda_n K \frac{\partial^2 p_c}{\partial (s_E^{l_s})^2} \varphi_E^{l_s} \nabla s_n \cdot \nabla \varphi_E^{k_p} + \int_E \lambda_n K \frac{\partial p_c}{\partial s_E^{l_s}} \nabla \varphi_E^{l_s} \cdot \nabla \varphi_E^{k_p}. \end{aligned}$$

Interior edges :

$$\frac{\partial G_{E_1}^{k_p}}{\partial p_{E_1}^{l_p}} = \frac{1}{2} \int_e -\lambda_t^1 K^1 \nabla \varphi_{E_1}^{l_p} \cdot n_e \varphi_{E_1}^{k_p} + \lambda_t^1 K^1 \nabla \varphi_{E_1}^{k_p} \cdot n_e \varphi_{E_1}^{l_p} + \frac{\sigma_e^0}{|e|^\beta} \int_e \varphi_{E_1}^{l_p} \varphi_{E_1}^{k_p}.$$

$$\begin{aligned}
\frac{\partial G_{E_1}^{k_p}}{\partial s_{E_1}^{l_s}} &= -\frac{1}{2} \int_e \frac{\partial \lambda_t^1}{\partial s_{E_1}^{l_s}} \varphi_{E_1}^{l_s} K^1 \nabla p_w^1 \cdot n_e \varphi_{E_1}^{k_p} - \frac{1}{2} \int_e \frac{\partial \lambda_n^1}{\partial s_{E_1}^{l_s}} \varphi_{E_1}^{l_s} K^1 \nabla p_c^1 \cdot n_e \varphi_{E_1}^{k_p} \\
&\quad - \frac{1}{2} \int_e \lambda_n^1 K^1 \frac{\partial^2 p_c^1}{\partial (s_{E_1}^{l_s})^2} \varphi_{E_1}^{l_s} \nabla s_{E_1} \cdot n_e \varphi_{E_1}^{k_p} - \frac{1}{2} \int_e \lambda_n^1 K^1 \frac{\partial p_c^1}{\partial s_{E_1}^{l_s}} \nabla \varphi_{E_1}^{l_s} \cdot n_e \varphi_{E_1}^{k_p} \\
&+ \frac{1}{2} \int_e \frac{\partial \lambda_t^1}{\partial s_{E_1}^{l_s}} \varphi_{E_1}^{l_s} K^1 \nabla \varphi_{E_1}^{k_p} \cdot n_e (p_w^1 - p_w^2) + \frac{1}{2} \int_e \frac{\partial \lambda_n^1}{\partial s_{E_1}^{l_s}} \varphi_{E_1}^{l_s} K^1 \nabla \varphi_{E_1}^{k_p} \cdot n_e (p_c^1 - p_c^2) \\
&\quad + \frac{1}{2} \int_e \lambda_n^1 \frac{\partial p_c^1}{\partial s_{E_1}^{l_s}} K^1 \nabla \varphi_{E_1}^{k_p} \cdot n_e \varphi_{E_1}^{l_s} + \frac{\sigma_e^0}{|e|^\beta} \int_e \frac{\partial p_c^1}{\partial s_{E_1}^{l_s}} \varphi_{E_1}^{l_s} \varphi_{E_1}^{k_p}.
\end{aligned}$$

$$\frac{\partial G_{E_2}^{k_p}}{\partial p_{E_2}^{l_p}} = -\frac{1}{2} \int_e \lambda_t^2 K^2 \nabla \varphi_{E_2}^{l_p} \cdot n_e \varphi_{E_2}^{k_p} + \lambda_t^1 K^1 \nabla \varphi_{E_1}^{k_p} \cdot n_e \varphi_{E_2}^{l_p} - \frac{\sigma_e^0}{|e|^\beta} \int_e \varphi_{E_2}^{l_p} \varphi_{E_2}^{k_p}.$$

$$\begin{aligned}
\frac{\partial G_{E_2}^{k_p}}{\partial s_{E_2}^{l_s}} &= -\frac{1}{2} \int_e \frac{\partial \lambda_t^2}{\partial s_{E_2}^{l_s}} \varphi_{E_2}^{l_s} K^2 \nabla p_w^2 \cdot n_e \varphi_{E_2}^{k_p} - \frac{1}{2} \int_e \frac{\partial \lambda_n^2}{\partial s_{E_2}^{l_s}} \varphi_{E_2}^{l_s} K^2 \nabla p_c^2 \cdot n_e \varphi_{E_2}^{k_p} \\
&\quad - \frac{1}{2} \int_e \lambda_n^2 K^2 \frac{\partial^2 p_c^2}{\partial (s_{E_2}^{l_s})^2} \varphi_{E_2}^{l_s} \nabla s_{E_2} \cdot n_e \varphi_{E_2}^{k_p} - \frac{1}{2} \int_e \lambda_n^2 K^2 \frac{\partial p_c^2}{\partial s_{E_2}^{l_s}} \nabla \varphi_{E_2}^{l_s} \cdot n_e \varphi_{E_2}^{k_p} \\
&\quad - \frac{1}{2} \int_e \lambda_n^1 \frac{\partial p_c^2}{\partial s_{E_2}^{l_s}} K^1 \nabla \varphi_{E_1}^{k_p} \cdot n_e \varphi_{E_2}^{l_s} - \frac{\sigma_e^0}{|e|^\beta} \int_e \frac{\partial p_c^2}{\partial s_{E_2}^{l_s}} \varphi_{E_2}^{l_s} \varphi_{E_2}^{k_p}.
\end{aligned}$$

$$\frac{\partial G_{E_2}^{k_p}}{\partial p_{E_1}^{l_p}} = \frac{1}{2} \int_e \lambda_t^1 K^1 \nabla \varphi_{E_1}^{l_p} \cdot n_e \varphi_{E_2}^{k_p} + \frac{1}{2} \int_e \lambda_t^2 K^2 \nabla \varphi_{E_2}^{k_p} \cdot n_e \varphi_{E_1}^{l_p} - \frac{\sigma_e^0}{|e|^\beta} \int_e \varphi_{E_1}^{l_p} \varphi_{E_2}^{k_p}.$$

$$\begin{aligned}
\frac{\partial G_{E_2}^{k_p}}{\partial s_{E_1}^{l_s}} &= \frac{1}{2} \int_e \frac{\partial \lambda_t^1}{\partial s_{E_1}^{l_s}} \varphi_{E_1}^{l_s} K^1 \nabla p_w^1 \cdot n_e \varphi_{E_2}^{k_p} + \frac{1}{2} \int_e \frac{\partial \lambda_n^1}{\partial s_{E_1}^{l_s}} \varphi_{E_1}^{l_s} K^1 \nabla p_c^1 \cdot n_e \varphi_{E_2}^{k_p} \\
&\quad + \frac{1}{2} \int_e \lambda_n^1 K^1 \frac{\partial^2 p_c^1}{\partial (s_{E_1}^{l_s})^2} \varphi_{E_1}^{l_s} \nabla s_{E_1} \cdot n_e \varphi_{E_2}^{k_p} + \frac{1}{2} \int_e \lambda_n^1 K^1 \frac{\partial p_c^1}{\partial s_{E_1}^{l_s}} \nabla \varphi_{E_1}^{l_s} \cdot n_e \varphi_{E_2}^{k_p} \\
&\quad + \frac{1}{2} \int_e \lambda_n^2 \frac{\partial p_c^1}{\partial s_{E_1}^{l_s}} K^2 \nabla \varphi_{E_2}^{k_p} \cdot n_e \varphi_{E_1}^{l_s} - \frac{\sigma_e^0}{|e|^\beta} \int_e \frac{\partial p_c^1}{\partial s_{E_1}^{l_s}} \varphi_{E_1}^{l_s} \varphi_{E_2}^{k_p}.
\end{aligned}$$

$$\frac{\partial G_{E_2}^{k_p}}{\partial p_{E_2}^{l_p}} = \frac{1}{2} \int_e \lambda_t^2 K^2 \nabla \varphi_{E_2}^{l_p} \cdot n_e \varphi_{E_2}^{k_p} - \frac{1}{2} \int_e \lambda_t^1 K^1 \nabla \varphi_{E_1}^{k_p} \cdot n_e \varphi_{E_2}^{l_p} + \frac{\sigma_e^0}{|e|^\beta} \int_e \varphi_{E_2}^{l_p} \varphi_{E_2}^{k_p}$$

$$\begin{aligned}
\frac{\partial G_{E_2}^{k_p}}{\partial s_{E_2}^{l_s}} &= \frac{1}{2} \int_e \frac{\partial \lambda_t^2}{\partial s_{E_2}^{l_s}} \varphi_{E_2}^{l_s} K^2 \nabla p_w^2 \cdot n_e \varphi_{E_2}^{k_p} + \frac{1}{2} \int_e \frac{\partial \lambda_n^2}{\partial s_{E_2}^{l_s}} \varphi_{E_2}^{l_s} K^2 \nabla p_c^2 \cdot n_e \varphi_{E_2}^{k_p} \\
&\quad + \frac{1}{2} \int_e \lambda_n^2 K^2 \frac{\partial^2 p_c^2}{\partial (s_{E_2}^{l_s})^2} \varphi_{E_2}^{l_s} \nabla s_{E_2} \cdot n_e \varphi_{E_2}^{k_p} + \frac{1}{2} \int_e \lambda_n^2 K^2 \frac{\partial p_c^2}{\partial s_{E_2}^{l_s}} \nabla \varphi_{E_2}^{l_s} \cdot n_e \varphi_{E_2}^{k_p} \\
&+ \frac{1}{2} \int_e \frac{\partial \lambda_t^2}{\partial s_{E_2}^{l_s}} \varphi_{E_2}^{l_s} K^2 \nabla \varphi_{E_2}^{k_p} \cdot n_e (p_w^1 - p_w^2) + \frac{1}{2} \int_e \frac{\partial \lambda_n^2}{\partial s_{E_2}^{l_s}} \varphi_{E_2}^{l_s} K^2 \nabla \varphi_{E_2}^{k_p} \cdot n_e (p_c^1 - p_c^2) \\
&\quad - \frac{1}{2} \int_e \lambda_n^2 \frac{\partial p_c^2}{\partial s_{E_2}^{l_s}} K^2 \nabla \varphi_{E_2}^{k_p} \cdot n_e \varphi_{E_2}^{l_s} + \frac{\sigma_e^0}{|e|^\beta} \int_e \frac{\partial p_c^2}{\partial s_{E_2}^{l_s}} \varphi_{E_2}^{l_s} \varphi_{E_2}^{k_p}.
\end{aligned}$$

Boundary edges :

$$\begin{aligned}
\frac{\partial G_{E_1}^{k_p}}{\partial p_{E_1}^{l_p}} &= - \int_e \lambda_t^1 K^1 \nabla \varphi_{E_1}^{l_p} \cdot n_e \varphi_{E_1}^{k_p} + \int_e \lambda_t^1 K^1 \nabla \varphi_{E_1}^{k_p} \cdot n_e \varphi_{E_1}^{l_p} + \frac{\sigma_e^0}{|e|^\beta} \int_e \varphi_{E_1}^{l_p} \varphi_{E_1}^{k_p}. \\
\frac{\partial G_{E_1}^{k_p}}{\partial s_{E_1}^{l_s}} &= - \int_e \frac{\partial \lambda_t^1}{\partial s_{E_1}^{l_s}} \varphi_{E_1}^{l_s} K^1 \nabla p_w^1 \cdot n_e \varphi_{E_1}^{k_p} - \int_e \frac{\partial \lambda_n^1}{\partial s_{E_1}^{l_s}} \varphi_{E_1}^{l_s} K^1 \nabla p_c^1 \cdot n_e \varphi_{E_1}^{k_p} \\
&\quad - \int_e \lambda_n^1 K^1 \frac{\partial^2 p_c^1}{\partial (s_{E_1}^{l_s})^2} \varphi_{E_1}^{l_s} \nabla s_{E_1} \cdot n_e \varphi_{E_1}^{k_p} - \int_e \lambda_n^1 K^1 \frac{\partial p_c^1}{\partial s_{E_1}^{l_s}} \nabla \varphi_{E_1}^{l_s} \cdot n_e \varphi_{E_1}^{k_p} \\
&+ \int_e \frac{\partial \lambda_t^1}{\partial s_{E_1}^{l_s}} \varphi_{E_1}^{l_s} K^1 \nabla \varphi_{E_1}^{k_p} \cdot n_e (p_w^1 - p_w^{dir}) + \int_e \frac{\partial \lambda_n^1}{\partial s_{E_1}^{l_s}} \varphi_{E_1}^{l_s} K^1 \nabla \varphi_{E_1}^{k_p} \cdot n_e (p_c^1 - p_c(s^{dir})) \\
&\quad + \int_e \lambda_n^1 \frac{\partial p_c^1}{\partial s_{E_1}^{l_s}} K^1 \nabla \varphi_{E_1}^{k_p} \cdot n_e \varphi_{E_1}^{l_s} + \frac{\sigma_e^0}{|e|^\beta} \int_e \frac{\partial p_c^1}{\partial s_{E_1}^{l_s}} \varphi_{E_1}^{l_s} \varphi_{E_1}^{k_p}.
\end{aligned}$$

Contribution from the saturation equation (17):

Volume integrals :

$$\begin{aligned}
\frac{\partial G_E^{k_s}}{\partial p_E^{l_p}} &= \int_E \lambda_w K \nabla \varphi_E^{l_p} \cdot \nabla \varphi_E^{k_s}. \\
\frac{\partial G_E^{k_s}}{\partial s_E^{l_s}} &= - \frac{\phi}{\Delta t} \int_E \varphi_E^{l_s} \varphi_E^{k_s} + \int_E \frac{\partial \lambda_w}{\partial s_E^{l_s}} \varphi_E^{l_s} K \nabla p_E \cdot \nabla \varphi_E^{k_s}.
\end{aligned}$$

Interior edges :

$$\frac{\partial G_{E_1}^{k_s}}{\partial p_{E_1}^{l_p}} = - \frac{1}{2} \int_e \lambda_w^1 K^1 \nabla \varphi_{E_1}^{l_p} \cdot n_e \varphi_{E_1}^{k_s} + \frac{1}{2} \int_e \lambda_w^1 K^1 \nabla \varphi_{E_1}^{k_s} \cdot n_e \varphi_{E_1}^{l_p} + \frac{\sigma_e^0}{|e|^\beta} \int_e \varphi_{E_1}^{l_p} \varphi_{E_1}^{k_s}.$$

$$\frac{\partial G_{E_1}^{k_s}}{\partial s_{E_1}^{l_s}} = - \frac{1}{2} \int_e \frac{\partial \lambda_w^1}{\partial s_{E_1}^{l_s}} \varphi_{E_1}^{l_s} K^1 \nabla p_w^1 \cdot n_e \varphi_{E_1}^{k_s} + \frac{1}{2} \int_e \frac{\partial \lambda_w^1}{\partial s_{E_1}^{l_s}} \varphi_{E_1}^{l_s} K^1 \nabla \varphi_{E_1}^{k_s} \cdot n_e (p_w^1 - p_w^2).$$

$$\frac{\partial G_{E_1}^{k_s}}{\partial p_{E_2}^{l_p}} = - \frac{1}{2} \int_e \lambda_w^2 K^2 \nabla \varphi_{E_2}^{l_p} \cdot n_e \varphi_{E_1}^{k_s} - \frac{1}{2} \int_e \lambda_w^1 K^1 \nabla \varphi_{E_1}^{k_s} \cdot n_e \varphi_{E_2}^{l_p} - \frac{\sigma_e^0}{|e|^\beta} \int_e \varphi_{E_2}^{l_p} \varphi_{E_1}^{k_s}.$$

$$\frac{\partial G_{E_1}^{k_s}}{\partial s_{E_2}^{l_s}} = - \frac{1}{2} \int_e \frac{\partial \lambda_w^2}{\partial s_{E_2}^{l_s}} \varphi_{E_2}^{l_s} K^2 \nabla p_w^2 \cdot n_e \varphi_{E_1}^{k_s}.$$

$$\frac{\partial G_{E_2}^{k_s}}{\partial p_{E_1}^{l_p}} = \frac{1}{2} \int_e \lambda_w^1 K^1 \nabla \varphi_{E_1}^{l_p} \cdot n_e \varphi_{E_1}^{k_s} + \frac{1}{2} \int_e \lambda_w^2 K^2 \nabla \varphi_{E_2}^{k_s} \cdot n_e \varphi_{E_1}^{l_p} - \frac{\sigma_e^0}{|e|^\beta} \int_e \varphi_{E_1}^{l_p} \varphi_{E_2}^{k_s}.$$

$$\frac{\partial G_{E_2}^{k_s}}{\partial s_{E_1}^{l_s}} = \frac{1}{2} \int_e \frac{\partial \lambda_w^1}{\partial s_{E_1}^{l_s}} \varphi_{E_1}^{l_s} K^1 \nabla p_w^1 \cdot n_e \varphi_{E_2}^{k_s}.$$

$$\frac{\partial G_{E_2}^{k_s}}{\partial p_{E_2}^{l_p}} = \frac{1}{2} \int_e \lambda_w^2 K^2 \nabla \varphi_{E_2}^{l_p} \cdot n_e \varphi_{E_2}^{k_s} - \frac{1}{2} \int_e \lambda_w^2 K^2 \nabla \varphi_{E_2}^{k_s} \cdot n_e \varphi_{E_2}^{l_p} + \frac{\sigma_e^0}{|e|^\beta} \int_e \varphi_{E_2}^{l_p} \varphi_{E_2}^{k_s}.$$

$$\frac{\partial G_{E_2}^{k_s}}{\partial s_{E_2}^{l_s}} = \frac{1}{2} \int_e \frac{\partial \lambda_w^2}{\partial s_{E_2}^{l_s}} \varphi_{E_2}^{l_s} K^2 \nabla p_w^2 \cdot n_e \varphi_{E_2}^{k_s} + \frac{1}{2} \int_e \frac{\partial \lambda_w^2}{\partial s_{E_2}^{l_s}} \varphi_{E_2}^{l_s} K^2 \nabla \varphi_{E_2}^{k_s} \cdot n_e (p_w^1 - p_w^2).$$

Boundary edges :

$$\frac{\partial G_{E_1}^{k_s}}{\partial p_{E_1}^{l_p}} = - \int_e \lambda_w^1 K^1 \nabla \varphi_{E_1}^{l_p} \cdot n_e \varphi_{E_1}^{k_s} + \int_e \lambda_w^1 K^1 \nabla \varphi_{E_1}^{k_s} \cdot n_e \varphi_{E_1}^{l_p} + \frac{\sigma_e^0}{|e|^\beta} \int_e \varphi_{E_1}^{l_p} \varphi_{E_1}^{k_s}.$$

$$\frac{\partial G_{E_1}^{k_s}}{\partial s_{E_1}^{l_s}} = - \int_e \frac{\partial \lambda_w^1}{\partial s_{E_1}^{l_s}} \varphi_{E_1}^{l_s} K^1 \nabla p_w^1 \cdot n_e \varphi_{E_1}^{k_s} + \int_e \frac{\partial \lambda_w^1}{\partial s_{E_1}^{l_s}} \varphi_{E_1}^{l_s} K^1 \nabla \varphi_{E_1}^{k_s} \cdot n_e (p_w^1 - p_w^{dir}).$$

The choice of the initial guess for the Newton-Raphson algorithm (22) plays a crucial role for the convergence of the Newton iterates. For $i > 0$, the initial guess for the time step $i + 1$ is chosen as:

$$(\bar{p}_w^{i+1,0}, \bar{s}_n^{i+1,0}) = (\bar{p}_w^i, \bar{s}_n^i).$$

For the first time step, we construct a special initial guess. As was stated above the model problem with formulations (9) and (10) is subject to an initial condition on the saturation (12). Therefore at time $i = 0$ we define

$$s_n^{1,0} = s^0, \quad (23)$$

and we choose for initial guess for the pressure $p_w^{1,0}$ the solution to the linear system of equations:

$$\begin{aligned} & \sum_E \int_E \lambda_t^0 K \nabla p_w^{1,0} \cdot \nabla z - \sum_{e \in \Gamma_h \cup \Gamma_{D^+} \cup \Gamma_{D^-}} \int_e \{ \lambda_t^0 K \nabla p_w^{1,0} \cdot n_e \} [z] \\ & + \sum_{e \in \Gamma_h \cup \Gamma_{D^+} \cup \Gamma_{D^-}} \int_e \{ \lambda_t^0 K \nabla z \cdot n_e \} [p_w^{1,0}] + \sum_{e \in \Gamma_h \cup \Gamma_{D^+} \cup \Gamma_{D^-}} \frac{\sigma_e^0}{|e|^\beta} \int_e [p_w^{1,0}] [z] \\ = & \sum_{e \in \Gamma_{D^+} \cup \Gamma_{D^-}} \int_e \lambda_t^0 K \nabla z \cdot n_e p_w^{dir} + \sum_{e \in \Gamma_{D^+} \cup \Gamma_{D^-}} \frac{\sigma_e^0}{|e|^\beta} \int_e p_w^{dir} z + \sum_E \int_E (q_w + q_n) z - \sum_E \int_E \lambda_n^0 K \nabla p_c^0 \cdot \nabla z \\ & + \sum_{e \in \Gamma_h \cup \Gamma_{D^-}} \int_e \{ \lambda_n^0 K \nabla p_c^0 \cdot n_e \} [z] - \sum_{e \in \Gamma_h \cup \Gamma_{D^-}} \int_e \{ \lambda_n^0 K \nabla z \cdot n_e \} [p_c^0] \\ - & \sum_{e \in \Gamma_h \cup \Gamma_{D^-}} \frac{\sigma_e^0}{|e|^\beta} \int_e [p_c^0] [z] + \sum_{e \in \Gamma_{D^-}} \int_e \lambda_n^0 K \nabla z \cdot n_e p_c^{dir} + \sum_{e \in \Gamma_{D^-}} \frac{\sigma_e^0}{|e|^\beta} \int_e p_c^{dir} z, \quad \forall z \in \mathcal{D}_{r_p}(\mathcal{E}_h). \end{aligned}$$

5 Numerical Simulations

We consider a square domain $\Omega = (0, 100)^2$ divided into a uniform grid of square cells. We refer to the mesh h_1 the mesh consisting of cells of side equal to $25m$, the mesh h_2 for cells of side equal to $12.5m$ and the mesh h_3 for cells of side equal to $6.25m$. Water and oil are the wetting phase and non-wetting phase respectively. The inflow and outflow boundaries and the fluid characteristics are given below:

$$\begin{aligned} \Gamma_- &= \{0\} \times (0, 100), & \Gamma_+ &= \{100\} \times (0, 100), \\ s_n^{dir} &= 0.15, & p_{dir}^- &= 3.e^6, & p_{dir}^+ &= 1.e^6, \\ \rho_w = \rho_n &= 1000kg/m^3, & \mu_n &= 0.01kg/ms, & \mu_w &= 0.001kg/ms, & \phi &= 0.2, & p_d &= 1.e^3Pa. \end{aligned}$$

Finally, we assume that $\beta = 1$ and $\Delta t = 1$ day. We consider both homogeneous and heterogeneous porous media. In the rest of the paper, we present pictures of the approximations of the water pressure and water saturation. We recall that $s_w = 1 - s_n$.

5.1 The homogeneous porous medium

We set the permeability $K = kI$ with $k = 5.e^{-8}$ over the entire domain. The pressure is approximated by piecewise quadratics and saturation by piecewise linears. The Brooks-Corey parameter θ is chosen equal to 2.

First we consider the DG scheme for the first formulation (9). The penalty parameter σ_e^0 in (16), (17) is set to 1.0. The numerical convergence of the approximations of pressure and saturation at 300 and 450 days is shown in Fig. 1 and Fig. 2. It only takes 4 Newton iterations at each time step for convergence of the Newton-Raphson scheme applied to (16), (17). This is true for all the test cases unless specified otherwise. We also recall that no slope limiting techniques are used.

Next, we vary the penalty parameter $\sigma_e^0 \in \{0.1, 1, 10\}$ and show the profiles of pressure and saturation at time $t = 450$ days in Fig. 3. There is no difference in the solutions for the method (9) as it can be seen from the figures; all profiles coincide. However, setting the penalty parameter σ_e^0 to zero in (16), (17) results in overshoot in saturation, which becomes greater than 1 at time step $t = 80$ days.

Second we compare the DG schemes for both formulations (9) and (10). The method (18), (19) is very sensitive with respect to the size of the penalty parameter. If σ_e^0 is chosen to be greater than 0.01, numerical overshoot occurs and saturation is greater than 1 at first time step. Fig. 4 and Fig. 5 contain comparisons of pressure and saturation profiles at 450 days obtained on meshes

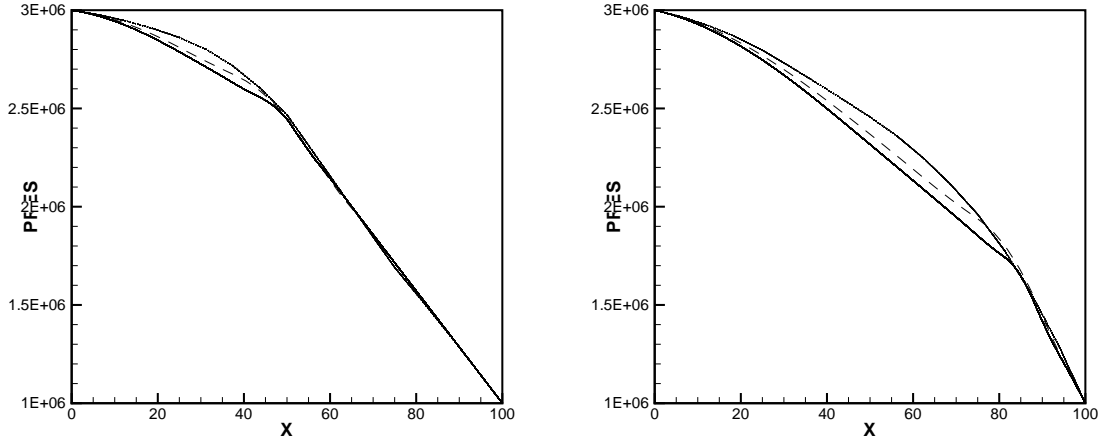


Fig. 1. Pressure profile ($r_p = 2, r_s = 1$) at 300 days (left) and 450 days (right) on meshes h_1 (dotted line), h_2 (dashed line) and h_3 (solid line) for penalty size $\sigma_e^0 = 1$.

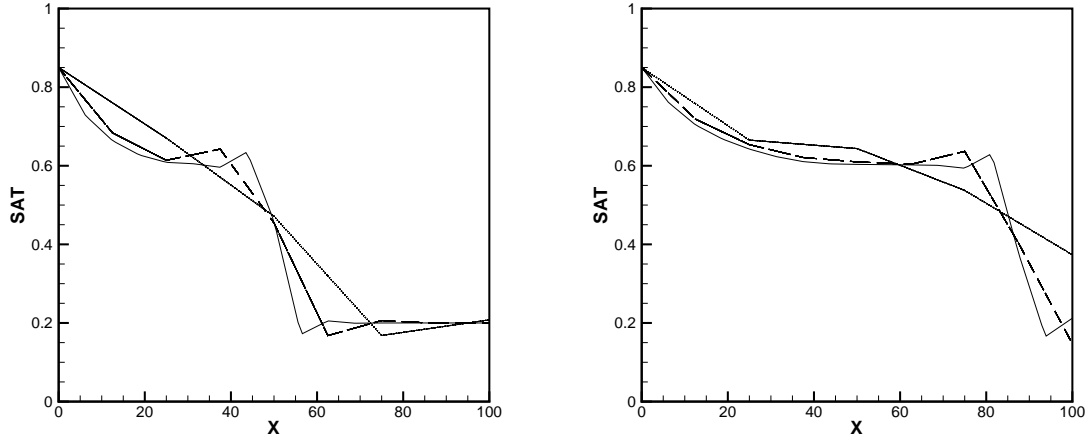


Fig. 2. Saturation profile ($r_p = 2, r_s = 1$) at 300 days (left) and 450 days (right) on meshes h_1 (dotted line), h_2 (dashed line) and h_3 (solid line) for penalty size $\sigma_e^0 = 1.0$.

h_2 and h_3 for a penalty parameter equal to 0.01. In this case, formulation (9) produces a sharper front than formulation (10).

Again, only 4 Newton iterations are needed at each time step for convergence of the Newton-Raphson scheme applied to (16), (17) and (18),(19) with penalty parameter equal to 0.01.

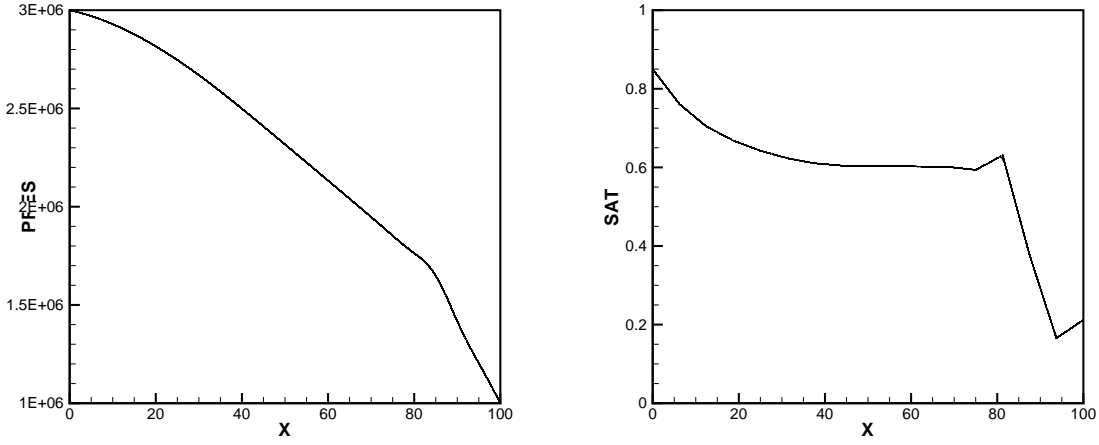


Fig. 3. Pressure (left) and saturation (right) profiles at 450 days on mesh h_3 , $r_p = 2$, $r_s = 1$, with penalty size $\sigma_e^0 = 0.1$ (dotted line), $\sigma_e^0 = 1.0$ (solid line) and $\sigma_e^0 = 10.0$ (dashed line).

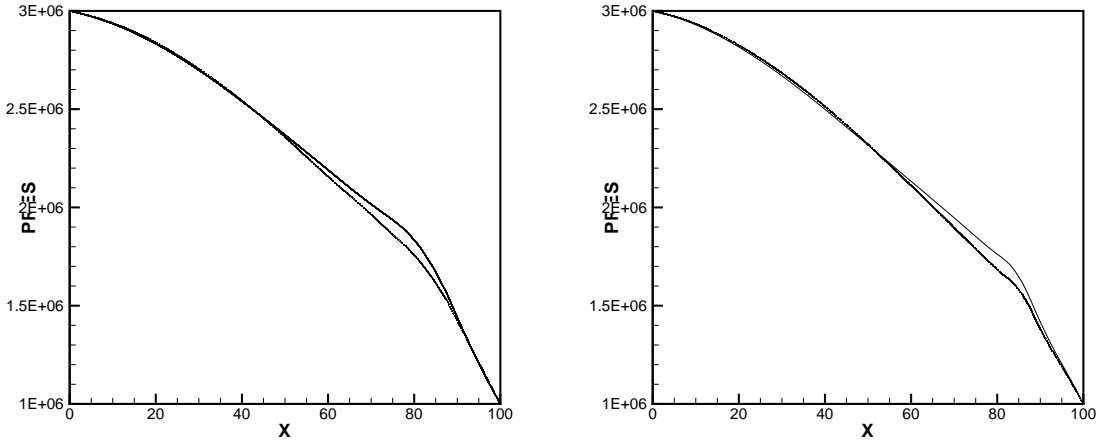


Fig. 4. Comparison of the pressure profile ($r_p = 2$, $r_s = 1$) for the two formulations at 450 days on meshes h_2 and h_3 for penalty size $\sigma = 0.01$: solid line for formulation (9) and dashed line for formulation (10).

5.2 The heterogeneous porous medium

We consider the heterogeneous permeability $K = kI$ with $k = 5.e - 8$ in most of the domain except in an inclusion where $k = 5.e - 12$ (see Fig. 6). The inclusion is located at $(37.5, 75) \times (25, 75)$. The Brooks-Corey parameter θ is chosen equal to 3. We fix the mesh $h = h_2$ and we vary the polynomial degrees for pressure and saturation approximations.

First, we show the evolution of pressure and saturation contours obtained

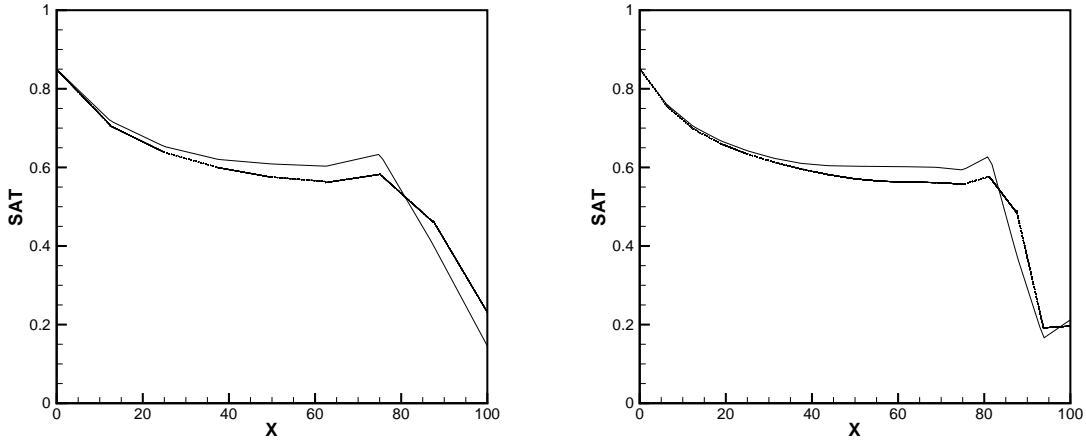


Fig. 5. Comparison of the saturation profile ($r_p = 2$, $r_s = 1$) for the two formulations at 450 days on meshes h_2 and h_3 for penalty size $\sigma = 0.01$: solid line for formulation (9) and dashed line for formulation (10).

with (16), (17) from 150 days to 450 days in Fig. 7 and Fig. 8. In this case, the pressure is approximated by quartic polynomials and the saturation by quadratic polynomials. The penalty parameter is equal to 1. Both pressure and saturation contours take into account the heterogeneity of the permeability field; the low permeability region acts as an impermeable zone where the wetting phase saturation does not penetrate.

Second, we show numerical convergence of (16), (17) by increasing the polynomial orders:

- Case 1: Piecewise cubics for pressure and piecewise linears for saturation: $r_p = 3$, $r_s = 1$.
- Case 2: Piecewise quartics for pressure and piecewise quadratics for saturation: $r_p = 4$, $r_s = 2$.
- Case 3: Piecewise polynomials of fifth degree for pressure and piecewise cubics for saturation: $r_p = 5$, $r_s = 3$.

The pressure and saturation contours at 300 and 550 days for the p-version are shown in Fig. (9), (10), (11) and Fig. (12), (13), (14). For the first case, the water floods the domain as if it was homogeneous. The accuracy of the solutions is greatly improved in cases 2 and 3.

Finally, we demonstrate that different penalties yield the same approximate solution. The profiles of saturation and pressure along the line $(0, 100) \times \{50\}$ are shown in Fig. 15. Here, the discrete orders are $r_p = 4$ and $r_s = 2$, but this result is also true for other choices of polynomial degrees.

As for the homogeneous case, it takes 4 newton iterations at each time step

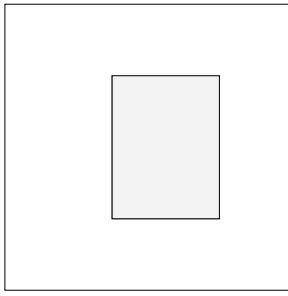


Fig. 6. Heterogeneous permeability field.

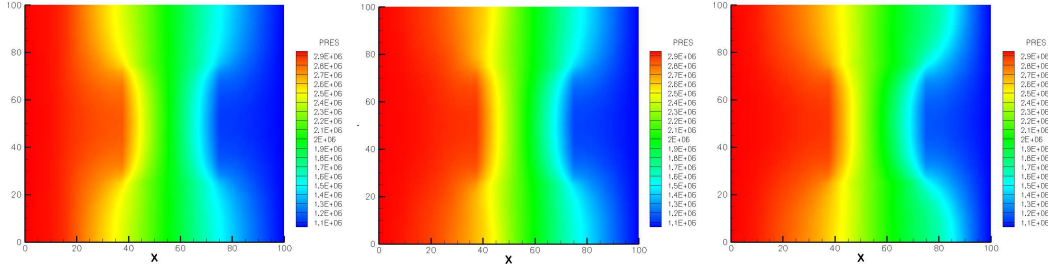


Fig. 7. Evolution of the pressure contour for $k_p = 4$, $k_s = 2$, on mesh h_2 at 150, 300 and 450 days for penalty $\sigma_e^0 = 1.0$.

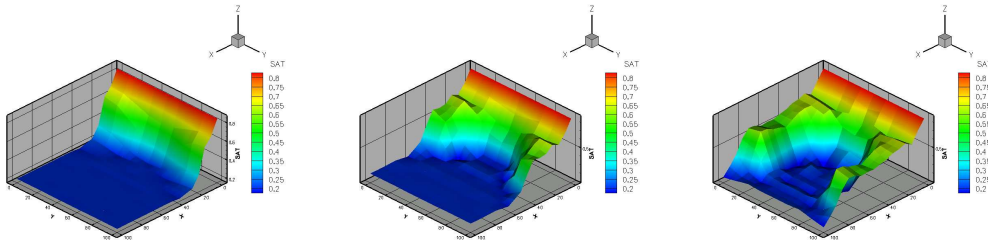


Fig. 8. Evolution of the saturation contour for $k_p = 4$, $k_s = 2$, on mesh h_2 at 150, 300 and 450 days for penalty $\sigma_e^0 = 1.0$.

to converge and no slope limiter techniques are applied.

The DG scheme applied to the second formulation (10) is again very sensitive to the choice of the penalty parameter. We observe numerically that approximations of pressure and saturation with polynomials degrees higher than 1 produce an increasing number of Newton-Rapshon iterations at each time step; eventually the iterations fail to converge. If one uses linears for both saturation and pressure spaces, one needs to use a very fine mesh in order to capture the heterogeneity and thus, computations become expensive.

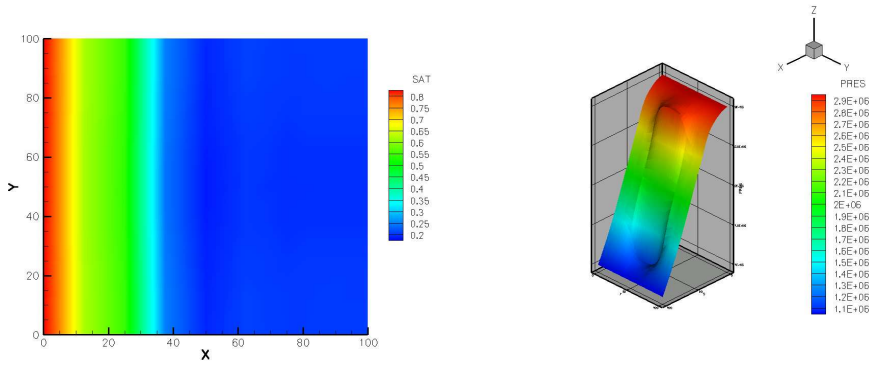


Fig. 9. Saturation and pressure contours on mesh h_2 for $k_p = 3$ and $k_s = 1$ at 300 days for penalty $\sigma_0^e = 1.0$.

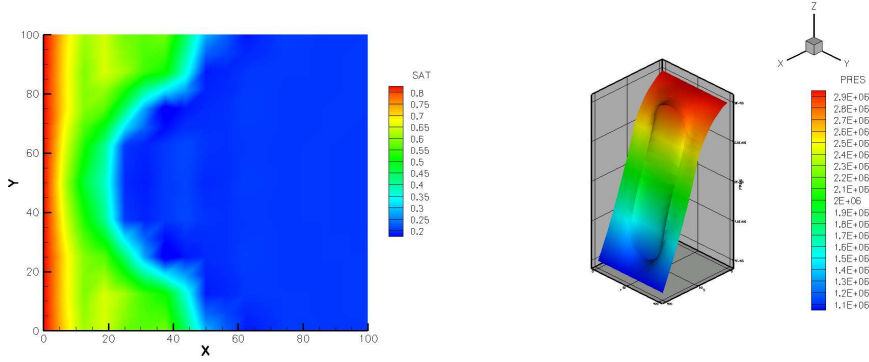


Fig. 10. Saturation and pressure contours on mesh h_2 for $k_p = 4$ and $k_s = 2$ at 300 days for penalty $\sigma_0^e = 1.0$.

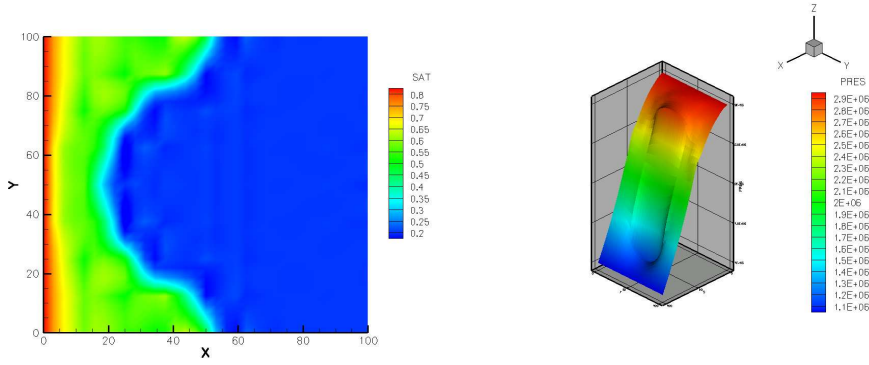


Fig. 11. Saturation and pressure contours on mesh h_2 for $k_p = 5$ and $k_s = 3$ at 300 days for penalty $\sigma_0^e = 1.0$.

6 Conclusions

In this paper, we present two high-order numerical methods based on two different formulations of two-phase flow. Due to their local features, the schemes are well-suited for heterogeneities such as discontinuous permeability fields

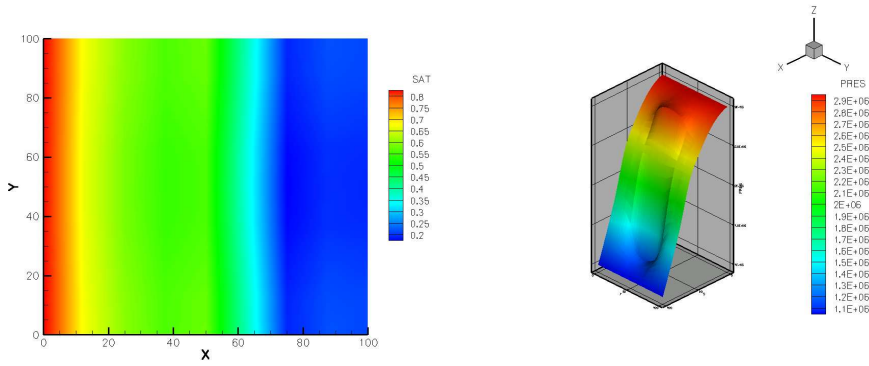


Fig. 12. Saturation and pressure contours on mesh h_2 for $k_p = 3$ and $k_s = 1$ at 550 days for penalty $\sigma_0^\epsilon = 1.0$.

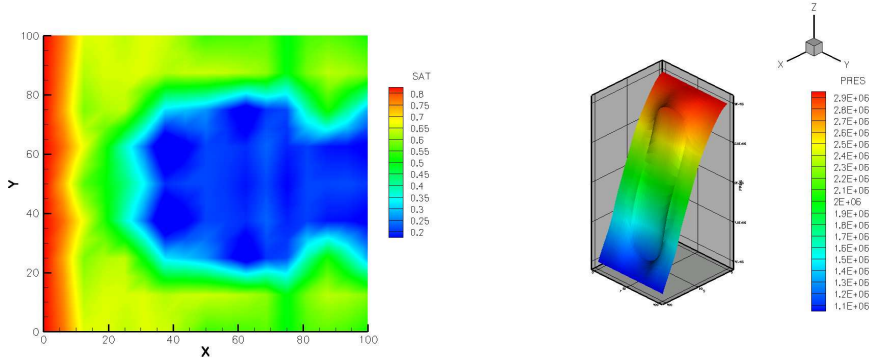


Fig. 13. Saturation and pressure contours on mesh h_2 for $k_p = 4$ and $k_s = 2$ at 550 days for penalty $\sigma_0^\epsilon = 1.0$.

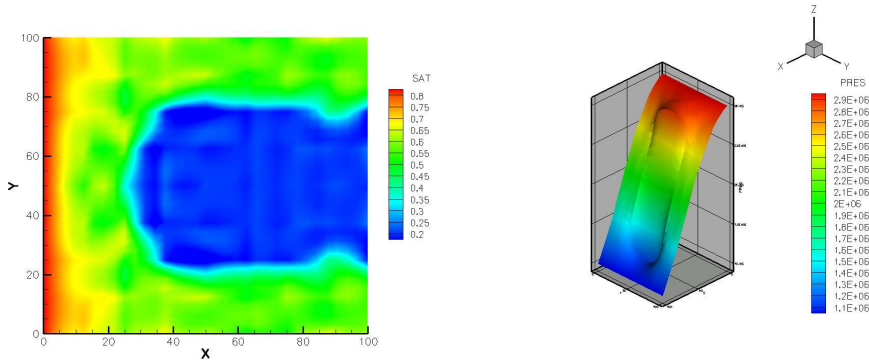


Fig. 14. Saturation and pressure contours on mesh h_2 for $k_p = 5$ and $k_s = 3$ at 550 days for penalty $\sigma_0^\epsilon = 1.0$.

and complex geometries. We show convergence of the numerical solutions by either refining the mesh successively or by increasing the polynomial degrees. We also demonstrate that for the first method, the size of the penalty parameter does not influence the solutions.

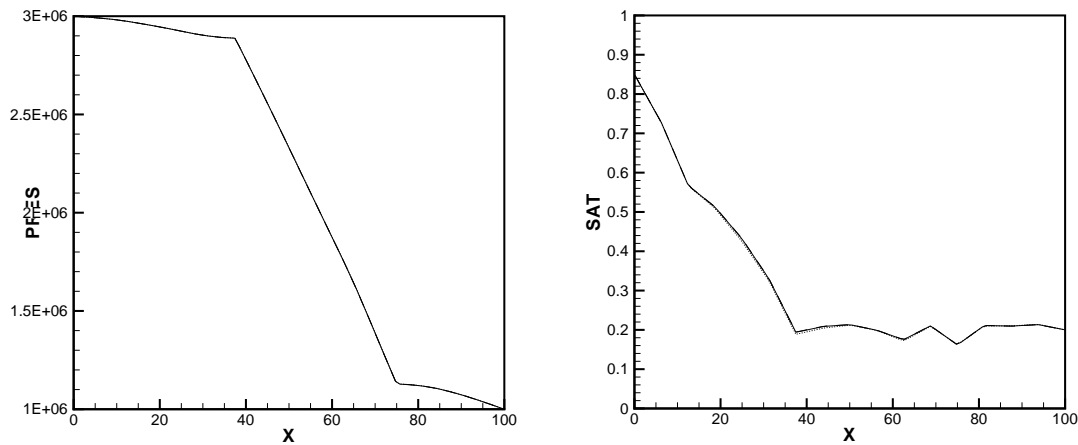


Fig. 15. Pressure and saturation profiles at 550 days on mesh h_2 for $k_p = 4$, $k_s = 2$ with penalties $\sigma_0^e = 0.1$ (dotted line), $\sigma_0^e = 1.0$ (solid line), $\sigma_0^e = 10.0$ (dashed line).

References

- [1] P. Bastian and B. Rivière. Discontinuous Galerkin methods for two-phase flow in porous media. Technical Report 2004-28, University of Heidelberg, 2004.
- [2] R.H. Brooks and A.T. Corey. Hydraulic properties of porous media. *Hydrol. Pap.*, 3, 1964.
- [3] G. Chavent and J. Jaffré. *Mathematical models and finite elements for reservoir simulation*. Studies in Mathematics and its Applications. 1986.
- [4] B. Cockburn, G.E. Karniadakis, and C.-W. Shu, editors. *First International Symposium on Discontinuous Galerkin Methods*, volume 11 of *Lecture Notes in Computational Science and Engineering*. Springer-Verlag, 2000.
- [5] B. Cockburn and C.W. Shu. TVB Runge-Kutta local projection discontinuous Galerkin finite element method for conservative laws II: General framework. *Mathematics of Computation*, 52:411–435, 1989.
- [6] S.M. Hassanizadeh and R.J. Schotting, editors. *Miscible displacement in porous media*, Proceedings of the XIV International Conference on Computational Methods in Water Resources, 2002.
- [7] R. Helmig. *Multiphase flow and transport processes in the subsurface*. Springer, 1997.
- [8] R. Huber and R. Helmig. Multiphase flow in heterogeneous porous media: a classical finite element method versus an implicit pressure-explicit saturation-based mixed finite element-finite volume approach. *International Journal for Numerical Methods in Fluids*, 29:899–920, 1999.
- [9] H. Goldstine. *A History of Numerical Analysis*. Springer-Verlag, 1977.

- [10] C.T. Miller, G. Christakos, P.T. Imhoff, J.F. McBride, and J.A. Pedit. Multiphase flow and transport modeling in heterogeneous porous media: challenges and approaches. *Advances in Water Resources*, 21(2):77–120, 1998.
- [11] M. Peszynska, Q. Lu, and M.F. Wheeler. Coupling different numerical algorithms for two phase fluid flow. In J.R. Whiteman, editor, *MAFELAP Proceedings of the Mathematics of Finite Elements and Applications*, pages 205–214, 1999.
- [12] B. Rivière. The DGIMPES model in IPARS: discontinuous Galerkin for two-phase flow integrated in a reservoir simulator framework. Technical Report 02-29, Texas Institute for Computational and Applied Mathematics, 2002. Available at <http://www.ices.utexas.edu/reports/2002.html>.
- [13] B. Rivière and E. Jenkins. In pursuit of better models and simulations, oil industry looks to the math sciences. *SIAM News*, 35(1), 2002.
- [14] B. Rivière and M.F. Wheeler. Locally conservative algorithms for flow. In J. Whiteman, editor, *Proceedings of Mathematics of Finite Elements and Applications MAFELAP 1999*, pages 29–46. Elsevier, Amsterdam, 2000.
- [15] B. Rivière and M.F. Wheeler. Discontinuous Galerkin methods for flow and transport problems in porous media. *Communications in Numerical Methods in Engineering*, 18:63–68, 2002.
- [16] B. Rivière, M.F. Wheeler, and K. Banas. Part II. Discontinuous Galerkin method applied to a single phase flow in porous media. *Computational Geosciences*, 4:337–349, 2000.
- [17] B. Rivière, M.F. Wheeler, and V. Girault. Improved energy estimates for interior penalty, constrained and discontinuous Galerkin methods for elliptic problems. Part I. *Computational Geosciences*, 3:337–360, April 1999.